FINITE-ELEMENT-METHOD CALCULATION OF FLOW AND HEAT TRANSFER IN ELEMENTS OF PLATE EXCHANGERS

A. A. Mikhalevich, V. I. Nikolaev, and V. K. Fedosova

UDC 536.24:532.54

The finite-element method is used to solve a problem concerning the heat transfer through a wall separating two rectangular channels. Calculations are performed to establish the distributions of temperature, velocity, heat flux, shear stress, and Nusselt number on the walls of the channels.

Introduction. The use of plate finning in heat exchangers makes it possible to achieve a high level of efficiency and equipment compactness while keeping hydraulic resistance comparatively low (relative to the flow across the fins).

A wide range of different types of surfaces are used in the construction of plate heat exchangers. The design of such units is presently based on the use of criterional (empirical) relations obtained from generalizations of experimental measurements. The simplicity of this approach and the long tradition of its use account for its popularity. However, one of the problems encountered here is the long time needed to obtain experimental information in the design of new units and the relatively high cost of this design work. An alternative approach to the solution of this problem is numerical modeling based on the solution of base transport equations for transport processes. The creation of a new generation of powerful computers is making it possible to use highly efficient numerical methods to satisfactorily model complex physical processes occurring in heat exchangers. The use of numerical methods has become so widespread that it is difficult to find an area of scientific inquiry where they are not employed.

In the present study, we attempt a direct through calculation of the temperatures and velocities in an element of a parallel-flow plate exchanger. The channel being modeled is shown in Fig. 1 and is represented by a system of two parallel rectangular channels (which, in the general case, have different geometric dimensions). The use of the mathematical model and the application package (HEATEX) based on it make it possible to design a system of channels with independent flows of a heat-transfer agent having certain thermophysical properties and certain initial and boundary conditions. The thermal part of the problem will be solved in a conjugate formulation, which precludes inaccuracies and errors in assigning the thermal boundary conditions on the washed part of the perimeter of the channels.

Before proceeding to the base equations, we should note that the program was realized on the basis of the finite-element method (FEM) and that it makes it possible to calculate the fields of velocity, temperature, and concentration in individual channels and units of different geometry (bundles of finned tubes, annular, rectangular, and axisymmetric channels, etc.) [1-3].

Flow Scheme and Initial Equations. The region of integration contains two parallel channels separated by a partition. Heat exchange takes place between the channels. In the general case, both exothermic and endothermic reactions can take place in the heat exchangers. We will examine an incompressible Newtonian fluid and use the assumptions normally employed in the absence of thermal and barodiffusion. The system of transport equations includes the equations of motion, energy, heat conduction in the wall, diffusion, and continuity. With the use of matrix notation, this system can be written as follows:

$$\rho \bar{U}_j \frac{\partial \bar{U}_i}{\partial x_j} = \frac{\partial}{\partial x_j}\left(\mu \frac{\partial \bar{U}_i}{\partial x_j} - \overline{\rho u_i' u_j'}\right) - \frac{\partial \bar{P}}{\partial x_i}; \quad (1)$$

Institute of Nuclear Power Engineering, Academy of Sciences of the Belorussian SSR, Minsk. Translated from Inzhenerno-Fizicheskii Zhurnal, Vol. 59, No. 5, pp. 747-757, November, 1990. Original article submitted October 16, 1989.

 0022-0841/90/5905-1380$12.50 © 1990 Plenum Publishing Corporation

$$\rho\bar{U}_j \frac{d\bar{T}}{\partial x_j} = \frac{\partial}{\partial x_j}\left(\frac{\mu}{\mathrm{Pr}} \frac{\partial \bar{T}}{\partial x_j} - \overline{\rho u_i' T'}\right) + \Theta_R; \tag{2}$$

$$\frac{\partial \bar{T}}{\partial x_j}\left(\lambda \frac{\partial \bar{T}}{\partial x_j}\right) + \Theta_i = 0; \tag{3}$$

$$\rho\bar{U}_j \frac{\partial \bar{C}}{\partial x_j} = \frac{\partial}{\partial x_j}\left(\frac{\mu}{\mathrm{Pr}_D} \frac{\partial \bar{C}}{\partial x_j} - \overline{\rho u_i' C'}\right) + \dot{I}_R; \tag{4}$$

$$\int_s \rho\bar{U}_z ds = \text{const.} \tag{5}$$

We used standard notation in writing system (1-5). The source terms Θ_R, Θ_i, and I_R in Eqs. (2-4) describe the sources (sinks) of heat and mass due to chemical reactions, as well as internal heat releases (if such occur) in the solid wall and the partition. Although certain difficulties are encountered when such sources are calculated (these difficulties being related mainly to the presence of nonlinearity), they are not of a fundamental nature. The study [2] can serve as an example of the use of the program to calculate heat transfer in the presence of internal heat releases (chemical reactions). A mathematical model of heat transfer in a chemically reacting flow was examined in considerable detail in this study.

In certain cases (such as with the pressurized flow of an incompressible heat-transfer agent in a rectangular channel of constant cross section at large Reynolds numbers), the equation of motion can be solved for the longitudinal component of the velocity vector (i.e. can be converted to parabolic form with respect to the longitudinal coordinate) by considering that the transverse components of velocity are small but nonetheless nontrivial (otherwise, the left side of Eq. (1) would completely disappear). Such an approach makes it possible to significantly reduce the volume of calculation necessary, although it should be noted that no fundamental difficulties are encountered in the calculation of the transverse components of velocity.

We will use an iterative procedure (the Wegstein method) to calculate the source term in the equation of motion $\partial\bar{P}/\partial x_i$. The physical criterion of convergence will be the equation of continuity, which was more conveniently used in the integral form in our investigation.

Boundary Conditions. The computing process was based on the use of a system of equations cast in parabolic form with respect to the long axis of the channel. Thus, it is necessary to know the inlet profiles of the functions being studied. Most authors (including us) use uniform (planar) profiles at the inlet. Neumann conditions are assigned on the lines of symmetry. Conditions of attachment for velocity and compatibility conditions for the normal heat fluxes and temperatures are satisfied along the wetted perimeter for the energy equation. The simplicity of realizing the attachment conditions on the washed part of the perimeter makes it possible to easily model different types and configurations of channels. We provided for the use of thermal boundary conditions of the first, second, and third type, as well as mixed boundary conditions.

The program could be further improved in regard to the realization of the boundary conditions by employing the "wall law" for the equation of motion. This procedure is now widely used and makes it possible to avoid excessive crowding of the finite-element grid around the wall. In this case, instead of the Dirichlet boundary condition on the washed part of the perimeter, we use the Neumann condition. To calculate the shear stress

$$\tau_{wa} = \mu \left.\frac{\partial U}{\partial n}\right|_{wa} \tag{6}$$

we choose the empirical "wall law"

$$\frac{U}{U_\tau} = \frac{1}{\varkappa} \ln (y^+ E), \tag{7}$$

from which we easily obtain

$$\frac{\partial U}{\partial n_{wa}} = \frac{\tau_{wa}}{\mu} = \frac{U_\tau^2 \rho}{\mu}. \tag{8}$$

The empirical constants entering into (6-8): E = 9.37; κ = 0.417; $y^+ \simeq 50$–100.

Turbulence Model. The presence of the Reynolds stresses $-\rho u_i' u_j'$ introduces additional unknowns into system (1-5). Thus, closing equations are needed to determine them. The model developed by N. I. Buleev is sufficiently simple and convenient for channels of arbitrary cross section, this model being a variant of the Prandtl mixing-length models. To determine the components of the tensor of the turbulence stresses, we use the traditional gradient relation with averaged motion:

$$-\overline{\rho u_i' u_j'} = \varepsilon_M \left(\frac{\partial \bar{U}_j}{\partial x_i} + \frac{\partial \bar{U}_i}{\partial x_j} \right); \tag{9}$$

$$-\overline{\rho u_i' T'} = \varepsilon_H \frac{\partial \bar{T}}{\partial x_i}, \tag{10}$$

where ε_M and ε_H are the coefficients of eddy viscosity and diffusivity, respectively. The following expressions were presented in [4] for the determination of these coefficients:

$$\frac{\varepsilon_M}{\varepsilon} = 0{,}2 f_0(\eta) f_1(\eta) \gamma^*; \tag{11}$$

$$\frac{\varepsilon_H}{\varepsilon} = 0{,}2 f_0(\lambda\eta) f_1(\lambda\eta) \gamma^*; \tag{12}$$

$$f_0(\eta) = \exp(-\eta); \tag{13}$$

$$f_1(\eta) = [1 - \exp(-\eta)]/\eta; \tag{14}$$

$$\eta = 65/\gamma^*; \tag{15}$$

$$\lambda = \begin{cases} 0{,}8 + 0{,}2/\mathrm{Pr}^{0,67}, & \mathrm{Pr} \leqslant 1, \\ 1, & \mathrm{Pr} > 1; \end{cases} \tag{16}$$

$$\gamma^* = \frac{L^2}{\gamma} \sqrt{\left(\frac{\partial \bar{U}_i}{\partial x_j} + \frac{\partial \bar{U}_j}{\partial x_i} \right)^2}, \tag{17}$$

where L is found from the relation

$$\frac{1}{L} = \frac{1}{2\pi} \int_0^{2\pi} \frac{1}{l(\varphi)} \, d\varphi. \tag{18}$$

The quantity $L(\phi)$ entering into Eq. (18) is the distance from the test point to the channel wall in the direction determined by the angle ϕ. It should be noted that analytical expressions for L have been obtained for through sections of certain characteristic geometries. For example, for a channel of rectangular cross section, the expression to determine the mixing length L has the form

$$\frac{1}{L} = \frac{1}{x_2 y_2 \sqrt{x_1^2 + y_1^2} + x_1 y_2 \sqrt{x_2^2 + y_1^2} + x_2 y_1 \sqrt{x_1^2 + y_2^2} + x_1 y_1 \sqrt{x_2^2 + y_2^2}}, \tag{19}$$

where x_1 and x_2 are the distances to the point M from one pair of opposite sides of the rectangle; y_1 and y_2 are the same for the other pair. There is currently no rigorous theory that makes it possible to calculate turbulent diffusion coefficients. They are usually found on the basis of the following relation:

$$\frac{D_t}{D} = \mathrm{Pr}_D \frac{\nu_t}{\nu}. \tag{20}$$

Numerical Method. To construct a discrete model, we subdivided the region into a finite number of elements which in aggregate approximate the form of the region we are studying. We then used the nodal values of the sought variable to construct a polynomial that determined the continuous quantity inside the element. The value of the continuous quantity at each nodal point was assumed to be variable and had to be determined.

An important feature of the finite-element method is that it can be used to efficiently solve nonlinear equations which describe processes in bodies of arbitrary form (or flow in channels of different configurations) with arbitrary boundary conditions.

We used linear and quadratic tetragons to solve the formulated problem. Such elements have second-order curves as boundaries. The value of the sought functions is determined at four or eight nodes located on the sides of the elements (Fig. 1). The number of elements into which the test region was subdivided was determined on the basis of considerations related to the optimum relationship between accuracy, computing time, and the speed of the computer. For example, we used 150-200 quadratic elements for the problem being studied here. System (1-5) can be represented by a single parabolic equation in which the coefficients with the derivatives take values corresponding to their physical significance. In other words, in the general case it is necessary to solve an equation of the following form:

$$G_1\frac{\partial\Phi}{\partial z}=\frac{\partial}{\partial x}\left(G_2\frac{\partial\Phi}{\partial x}\right)+\frac{\partial}{\partial y}\left(G_2\frac{\partial\Phi}{\partial y}\right)+\Theta. \tag{21}$$

Using the Galerkin method and the approximation in [5]:

$$\Phi(x,\ y)=\sum_{n=1}^{M}N_i(x,\ y)\,\Phi_i(z),$$

where M is the number of nodes in the element, we can write the condition expressing the orthogonality of the error relative to the basis functions:

$$\iint_{\Omega}N_i\left[\frac{\partial}{\partial x}\left(G_2\frac{\partial\Phi}{\partial x}\right)+\frac{\partial}{\partial y}\left(G_2\frac{\partial\Phi}{\partial y}\right)+\Theta-G_1\frac{\partial\Phi}{\partial z}\right]d\Omega=0. \tag{22}$$

Using Green's transformation for the first and second terms of the last formula, we obtain

$$\iint_{\Omega}G_2\left[\frac{\partial N_i}{\partial x}\frac{\partial\Phi}{\partial x}+\frac{\partial N_i}{\partial y}\frac{\partial\Phi}{\partial y}\right]d\Omega-\iint_{\Omega}N_i\Theta d\Omega+\iint_{\Omega}N_iG_1\frac{\partial\Phi}{\partial z}d\Omega-\int_{\Gamma}N_iqd\Gamma=0. \tag{23}$$

Integration is performed over the region of the elements, since in the remaining region (by definition) the basis functions N_i are equal to zero. Inserting the expression for $\Phi(x, y)$ into the last formula and using matrix notation, we write

$$[C]\frac{d\{\Phi\}}{dz}+[K]\{\Phi\}+\{F\}=0. \tag{24}$$

In this formula, as in all previous and subsequent calculations, we make use of the matrix notation normally employed in the FEM: damping matrix [C]; stiffness matrix [K]; gradient matrix [B]; load-vector matrix {F}. The expressions used to calculate these matrices for each element have the form:

$$[C]^{(e)}=\int_{\Omega}G_1[N]^{\mathrm{T}}[N]\,d\Omega; \tag{25}$$

$$[K]^{(e)}=\int_{\Omega}[B]^{\mathrm{T}}[D][B]\,d\Omega+\int_{S^2}\varkappa[N]^{\mathrm{T}}[N]\,dS; \tag{26}$$

$$\{F\}^{(e)}=-\int_{\Omega}\Theta[N]^{\mathrm{T}}\,d\Omega+\int_{S_1}q[N]^{\mathrm{T}}\,dS-\int_{S_2}\varkappa\Phi_{\infty}[N]^{\mathrm{T}}\,dS. \tag{27}$$

The global matrices for the entire ensemble are obtained by summing the contributions of the individual elements, which is done in the usual manner. It should be noted that, in the general case, the conductivity matrix [D] considers the anisotropy of the properties of the materials (medium) and for the heat-conduction equation (for example) has the form

$$[D]=\begin{vmatrix}\lambda_{xx}&0&0\\0&\lambda_{yy}&0\\0&0&\lambda_{zz}\end{vmatrix}. \tag{28}$$

Two approaches can be used to integrate over the axis: either the Galerkin procedure can be used for unidimensional elements along the z axis or a finite-difference approximation can be constructed along this axis. We used the second variant. Thus, integration over the flow was done in accordance with an implicit two-level scheme:

$$K_{i+1}\Phi_{i+1} + C_{i+1}(\Phi_{i+1} - \Phi_i)/\Delta z - F_{i+1} = 0. \tag{29}$$

The scheme is nonlinear and the iteration is performed in accordance with the following:

$$[K_{i+1}^{(s)} + C_{i+1}^{(s)}/\Delta z]\,\Phi_{i+1}^{(s+1)} = C_{i+1}^{(s)}\,\Phi_{i+1}^{(s)}/\Delta z + F_{i+1}^{(s)}. \tag{30}$$

Oscillations which develop during the computation can be eliminated if we simultaneously decrease the size of the elements and the step Δz. We employed an automatic step selection procedure. The steps were chosen using the standard deviation for two adjacent levels.

The system of algebraic equations was solved by Gauss' direct method, which is accurate to within the rounding error. To save memory, the matrices were converted to banded form.

It should be noted that the information obtained directly in the course of solving the system of initial equations, i.e. the local values of the sought functions at the nodes of the elements, was analyzed with the use of programs we developed. These programs made it possible to integrate local values along specified directions (along the wetted perimeter), differentiate at nodal points, determine the norms (standard deviations) for any step z_i, find and construct isolines of the sought functions, and determine averaged characteristics of the sought functions.

The generation of the initial data on the geometry of the region is important in the realization of the FEM. Although this matter is not of fundamental importance (and is thus rarely discussed in the literature), most errors arise during the compilation of the coordinate files and the so-called coupling matrices. In addition, manual compilation of these files is inefficient and time-consuming when there is a large number of elements. In connection with this, below we discuss one possible algorithm for automatic generation of the coordinates and coupling matrices for quadratic tetragonal elements. The algorithm can be used for both cartesian and polar coordinate systems.

Generation of a Grid of Elements. To construct the coordinate file CORD(I, J) (which in the FEM is most conveniently compiled as a file in which I is the number of the node and J is the index of the coordinate – equal to 1 if the X-coordinate is being filled out and equal to 2 for the Y-coordinate), we construct the vectors of the coordinate axes XM(I) and YM(I). The recursion formulas for determining the nodal coordinates have the form

$$XM(2*I) = X(I) + \frac{X(I+1) + X(I)}{2},$$

$$YM(2*I) = Y(I) + \frac{Y(I+1) + Y(I)}{2}$$

for the corner nodes and

$$XM(2*I-1) = X(I), \quad YM(2*I-1) = Y(I)$$

for the intermediate nodes on the sides of the elements.

The files X(I) and Y(I) which enter into these relations are the initial data. We then follow simple procedures to construct the two-dimensional files CORD X(I, J), CORD Y (I, J), which are filled by the "corner" and "side" files XM, YM. The two-dimensional files are then converted into files that are convenient for use in the FEM:

$$\left.\begin{aligned} CORD(K,\ 1) &= CORD\,X(I,\ J) \\ CORD(K,\ 2) &= CORD\,Y(I,\ J) \end{aligned}\right\} \rightarrow CORD(K,\ M),$$

$$K = 1,\ NEL,\quad M = 1,\ 2.$$

The index matrix is generated by means of the following cycles:

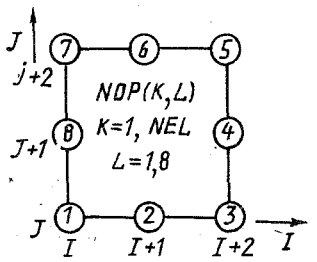

$$K = 1$$

$$DO \quad 1 \quad I = 1, \ LX\,2{,}2$$

$$DO \quad 1 \quad J = 1, \quad LY\,2{,}2$$

$$NOP\,(K,\ 1) = J + (LY + NY)\,(I - 1)/2$$

$$NOP\,(K,\ 8) = (J + 1) + (LY + NY)\,(I - 1)/2$$

$$NOP\,(K,\ 7) = (J + 2) + (LY + NY)\,(I - 1)/2$$

$$NOP\,(K,\ 3) = J + (LY + NY)\left(\frac{I - 1}{2} + 1\right)$$

$$NOP\,(K,\ 4) = (J + 1)\,(LY + NY)\left(\frac{I - 1}{2} + 1\right)$$

$$NOP\,(K,\ 5) = (J + 2) + (LY + NY)\left(\frac{I - 1}{2} + 1\right)$$

$$1. \ K = K + 1$$

$$K = 1$$

$$DO \ 2 \ I = 2, \ LX1, 2$$

$$DO \ 2 \ J = 1, \ MY$$

$$NOP\,(K,\ 2) = J + LY * \frac{I}{2} + NY\left(\frac{I}{2} - 1\right)$$

$$NOP\,(K,\ 6) = (J + 1) + LY * \frac{I}{2} + NY\left(\frac{I}{2} - 1\right)$$

$$2. \ K = K + 1$$

N_x is the number of nodes for X

N_y is the number of nodes for Y

$$LX = 2 * NX - 1$$

$$LY = 2 * NY - 1$$

$$LX\,2 = LX - 2$$

$$LY2 = LY - 2$$

$$LX\,1 = LX - 1$$

$$MY = NY - 1$$

Results and Discussion. As was noted above, we performed numerical calculations for a parallel-flow heat exchanger with two parallel rectangular channels (in the general case, we examined channels of different cross sections). Since the mathematical model made provision for the occurrence of either exothermic or endothermic reactions in the exchanger, we examined a case in which these reactions were present. On one side of the exchanger, the parameters of the heat-transfer agent are such that the chemical reactions occur at a high rate. On the other side, the parameters are such that the flow is nearly "frozen," i.e. the forward and reverse reactions are in thermodynamic equilibrium. Such a choice of parameters allowed us to study and compare the specific features of heat transfer in the presence of chemical reactions and in their absence.

Table 1 shows values of the thermohydraulic parameters of the heat-transfer agent at the inlet of the exchanger.

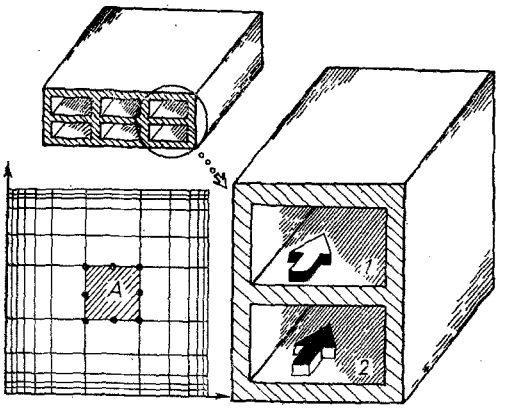

Fig. 1. Modeled element of heat exchanger; conditional subdivision of the region into finite elements; A – isoparametric square tetragon.

TABLE 1. Values of Geometric and Thermohydraulic Parameters

U_{in}, m/sec		T_{in}, K		Dimensions of sides of channels, m		Thickness of partition between channels, mm
channel I	channel II	I	II	I	II	
3	6	450	600	0,06×0,02	0,06×0,038	2

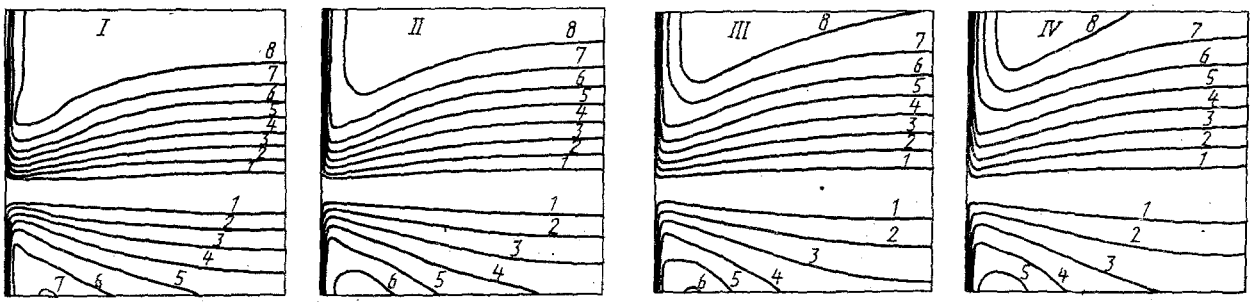

Fig. 2. Isolines of mean velocity U, m/sec, for channel sections different distances from the inlet (in the stabilization region): 1) 0.91; 2) 1.83; 3) 2.74; 4) 3.65; 5) 4.57; 6) 5.48; 7) 6.39; 8) 7.31; modes I-IV correspond to z/d = 1.0; 2.0; 3.0; 4.0.

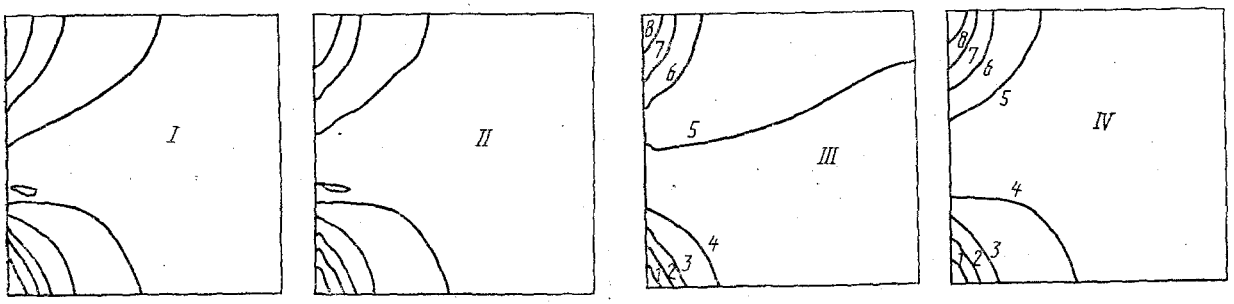

Fig. 3. Isotherm of averaged temperature T, K, for sections located different distances from the channel inlet: 1) 504.1; 2) 506.4; 3) 508.7; 4) 510.9; 5) 513.2; 6) 515.6; 7) 517.8; 8) 520.0; modes I-IV correspond to z/d = 1.0; 2.0; 3.0; 4.0.

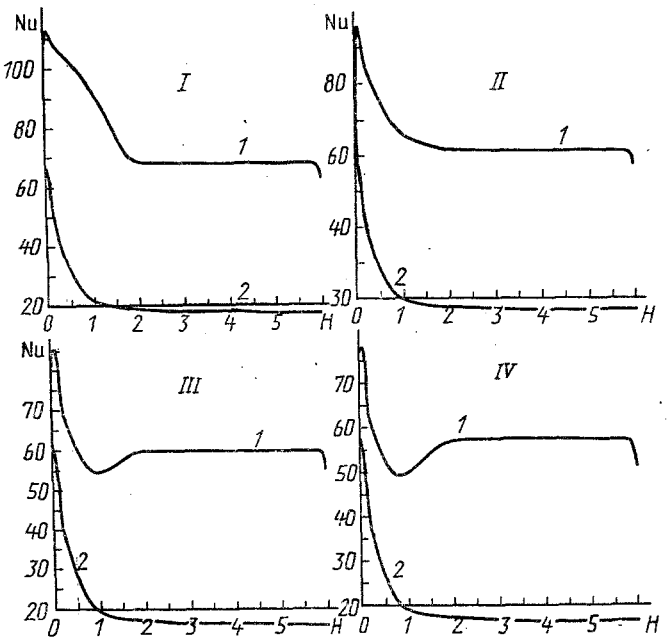

Fig. 4. Local Nusselt numbers on the hot (1) and cold (2) sides of the dividing wall; modes I-IV correspond to z/d = 1.0; 2.0; 3.0; 4.0.

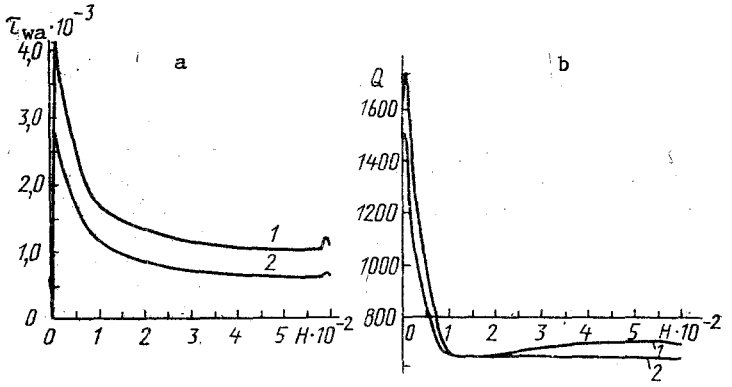

Fig. 5. Local shear stresses τ_{wa} (a) and heat flux Q (b) on the dividing wall on the sides where the heat-transfer agent is hot (1) and cold (2). Q, W/m^2; τ_{wa}, N/m^2; H, m.

The formation of the velocity and temperature profiles along the Z axis (downstream) is shown in Figs. 2 and 3, where modes I-IV correspond to sections different distances from the inlet. The velocity profile changes more rapidly around the thermally insulated (adiabatic) walls of the channels. It should be noted that distinct maxima are formed with increasing distance from the inlet (as is evident from Fig. 2), these maxima being localized around the sides of the channels adjacent to the partition. The shear stresses on the surface of the dividing (heat-transmitting) wall have peak-like maxima (Fig. 5a). The maximum shear stress is reached in the neighborhood of the interior right angle. The peak-like (nonsmooth) maxima are due to the fact that the theoretical symmetry cell (modeling the region of interest) was constructed with the use of mathematical right angles, i.e., angles without curvature. Such corner points are essentially singular points where the normal derivatives undergo a discontinuity.

In contrast to the case of velocity, calculation of the temperature profile is done with the use of homogeneous boundary conditions of the Neumann type (lines of symmetry and triviality of the normal derivatives at the boundaries of the region). Figure 4 shows the specifics of the heat transfer process in the given case of a chemically reactive heat carrier. The figure shows the distribution of the local Nusselt numbers along the dividing wall on the hot and cold sides of the wall, respectively.

The first two modes are characterized by qualitatively identical physical patterns and quantitative differences in heat transfer (which is understandable, since the top curve pertains to the hot channel and the bottom curve to the cold channel). However, the pattern then undergoes a qualitative change, and in modes III and IV there appear minima in the distribution of Nu on the hot-gas side near the corner regions (at the base of the partition). This development is due to stagnation of the flow in these regions and a consequent reduction in the rate of heat transfer. The lower curve pertains to the heat-transfer agent, where the reaction is "frozen" at the channel inlet. The qualitative behavior of the curve is no different from that of a corresponding inert heat carrier.

The same factors are responsible for the qualitative difference in the behavior of the curves of the distribution of heat flux along the corresponding sides of the partition (Fig. 5b).

In conclusion, we should note that the calculations were performed on an ES-1061 computer. Less than 1 min of processor time was used on each step. We used both service programs based on the Grafor system and "home-grown" (specific for the FEM) graphics programs for post-processor analysis of the results. The initial data was generated with a special module for automatic data preparation. The program was tested by the usual techniques — by using test functions and by comparison with experiments and analytical solutions.

NOTATION

$\overline{U}_i$, mean velocity in the i-th direction; u_i', fluctuations of velocity in the i-th direction; $\overline{C}$, mean concentration; $\overline{T}$, mean temperature; ρ, density; λ, thermal conductivity of the wall of the channels; μ, viscosity of the heat-transfer agent; Pr, Prandtl number; Pr_D, diffusional Prandtl number; Θ_R, source (sink) of heat due to chemical reactions; Θ_i, internal heat release in the channel walls; I_R, source (sink) of mass in the chemical reaction; S, cross section of channel; $\overline{P}$, mean pressure; n, normal vector.

LITERATURE CITED

1. V. I. Nikolaev, Turbulent Transport Processes in Reactive Systems (materials of an international school-seminar), Minsk (1985), pp. 128-139.
2. V. I. Nikolaev, V. A. Nemtsev, and L. N. Shegidevich, Izv. Akad. Nauk BelSSR Ser. Fiz. Energ. Nauk, No. 1, 43-47 (1987).
3. A. A. Mikhalevich and V. I. Nikolaev, Inzh. Fiz. Zh., 55, No. 2, 202-208 (1988).
4. N. I. Buleev, Heat Transfer [in Russian], Moscow (1962), pp. 64-98.